

Influence of Carbon Nanotubes on Polyamide Properties



This work is licensed under a Creative Commons Attribution 4.0 International License

S. Lučić Blagojević,* N. Šorgo, and Z. Buhin Šturlić

Faculty of Chemical Engineering and Technology,
University of Zagreb, Marulićev trg 19,
10000 Zagreb, Croatia

<https://doi/10.15255/CABEQ.2018.1567>

Original scientific paper
Received: December 21, 2018
Accepted: September 13, 2019

In this study, the addition of carbon nanotubes (MWCNT) and modified carbon nanotubes (MWCNT-COOH) in the range of 0.5 wt. % to 5 wt. % in polyamide (PA) obtained as a residue upon 3D printing, was investigated. PA and nanocomposite samples were prepared by melt mixing. PA/MWCNT and PA/MWCNT-COOH nanocomposites were characterized by differential scanning calorimetry (DSC), thermogravimetric analysis (TGA), THB thermal conductivity determination method, electrochemical impedance spectroscopy (EIS), and tensile test. Results of DSC analysis showed that both types of carbon nanotubes (MWCNTs) acted as nucleation centres of PA matrix, but had no effect on the order of the crystalline structure. Due to the polar nature of the surface and better dispersion, MWCNT-COOH filler accelerated PA crystallization more significantly compared to MWCNT. Due to the presence of nanofiller, the PA chains had limited motion space, which interfered with the crystallization process of the matrix. The thermal stability of the PA matrix increased with the addition of both MWCNT and MWCNT-COOH fillers. Higher thermal conductivity was achieved with the addition of MWCNT-COOH filler compared to the addition of MWCNT. The results of the tensile test showed that with the addition of both types of MWCNT fillers in the PA matrix, the modulus of elasticity and yield stress had reduced, but the yield strain increased. Results of the EIS showed that MWCNT nanofiller had not changed the electrical conductivity regardless of modification.

Keywords:

PA/MWCNT, PA/MWCNT-COOH, thermal properties, thermal stability, thermal conductivity, electrical conductivity, mechanical properties

Introduction

Over the last decades, polymer nanocomposites have attracted the attention of many scientists due to the ability to achieve improved and multifunctional properties. Among the investigated nanocomposites is a group of nanodimensional carbon allotropes such as graphene, fullerenes, and carbon nanotubes. Some research on these high-performance nanocomposites is focused on explaining their mechanical properties using molecular dynamics or dissipative particle dynamics^{1,2}, while others are aimed at innovative methods of production³.

Unlike single-walled carbon nanotubes (SWCNT), multi-walled carbon nanotubes (MWCNT) consist of two or more concentric cylindrical layers of graphene coaxially located around the central cavity. Because of its nanometric dimensions and structure, carbon nanotubes have specific thermal, electrical, and mechanical properties that depend on chirality, i.e., the way they are rolled. Therefore, CNTs represent a group of nanofillers

that can significantly improve polymer properties. However, carbon nanotubes tend to aggregate, which represents a problem in achieving uniform distribution in the polymer matrix. Various carbon-nanotube surface modifications enable the solution to this issue⁴.

Polyamides are technically important polymers of great significance for almost every industry. Polar amide groups have the ability to link the macromolecules' chains with strong hydrogen bonds. Therefore, polyamides are crystalline elastomers with high melting temperature, high thermal stability, high strength and toughness, and good resistance to various types of solvents that allow them extensive application⁵.

Polyamide 12 has a significant place in selective laser sintering (SLS) that is an additive manufacturing technique⁶. Polymeric materials for SLS are used in the form of a powder, and must meet a number of requirements, including thermal and optical properties, suitable viscosity and surface tension⁷. In addition, the shape and surface of the individual particles as well as the powder particle-size distribution are very important characteristics.

*Corresponding author: E-mail: slucic@fkit.hr

Therefore, during the production of PA 12 for SLS, the powder must be specially treated and adjusted to meet the requirements. A necessary condition for the SLS process is a sufficient sintering window (temperature difference between melting and crystallization) as well as a low zero viscosity and low surface tension⁷. In order to satisfy these conditions, the molecular structure and consequent properties of PA12 powder for SLS are significantly different from the conventional PA 12 for injection moulding⁷. Unfortunately, during the SLS process, the powder that is not an integral part of the printed 3D object undergoes some changes and after several printing cycles it becomes unusable for this purpose^{6–8}. Thus, significant efforts have been made in tailoring the structure and properties of materials for SLS, as well as exploring the possibility of using the valuable waste powder for other applications⁶.

Previous research has shown that the addition of carbon nanotubes can improve thermal, mechanical, and electrical properties of different polyamides, as well as their thermal stability^{9–18}. The aim of this study was to investigate the influence of the addition of multi-walled carbon nanotubes (MWCNT) and their modification (MWCNT-COOH) on thermal, electrical, and mechanical properties, and thermal stability of PA 2200. Taking into account the structural differences between PA 12 for SLS and other types of PA previously investigated, in this study, the polyamide 2200 (polyamide 12) obtained as a residue upon SLS was used. Therefore, the option of adding MWCNT nanofillers was investigated in order to explore the possibility of using the PA 2200 residue for other purposes.

Materials and methods

Materials

The materials used for the preparation of the nanocomposites were nanofillers: multi-walled carbon nanotubes (MWCNT) and oxidized multi-walled carbon nanotubes (MWCNT-COOH), manufactured by Chengdu Organic Chemicals Co. Ltd., China. Polyamide PA 2200, a type of PA 12 used as material for SLS, produced by EOS GmbH – Electro Optical Systems, is a fine polyamide powder with average grain size 56 μm and melting point 172 – 180 $^{\circ}\text{C}$. In this paper, the SLS PA 2200 waste powder supplied by Klex d.o.o., Croatia, was used as a matrix.

Preparation of PA/MWCNT nanocomposites

The samples of the PA nanocomposites were prepared by a melting process. A certain amount of nanofillers and polyamide for each sample was

weighed, and two different systems were prepared: PA/MWCNT and PA/MWCNT-COOH with 0.5 %, 1 %, 2 %, 3 %, 4 %, and 5 % mass fraction of the filler. The nanocomposite samples were mixed in a Brabender mixer for 3 min at a temperature of 200 $^{\circ}\text{C}$ and speed of 20 rpm. They were then homogenized for another 5 min at 60 rpm to ensure good dispersion of the filler. The samples were extracted individually from the mixer and manually trimmed. Chilled and chopped samples were pressed in a mould on a laboratory hydraulic press. The pressing was carried out in cycles: preheating for about 5 minutes, pressing for 7 minutes at 200 $^{\circ}\text{C}$ and 25 bars, and cooling with water to 120 $^{\circ}\text{C}$. The dimensions of the obtained samples were 100 x 100 x 1 mm.

Scanning electron microscopy

Dispersion of MWCNT and MWCNT-COOH fillers in PA matrix was investigated with scanning electron microscope (SEM), Tescan VEGA 3. Observations were made for PA composites with 5 % of MWCNT and MWCNT-COOH fillers on the area where a fracture occurred during the testing of mechanical properties.

Differential scanning calorimetry (DSC)

Thermal properties of the polyamide matrix (PA), PA/MWCNT, and PA/MWCNT-COOH nanocomposites were determined by differential scanning calorimetry under non-isothermal conditions. The tests were carried out on the Mettler Toledo DSC 823e instrument in a temperature range of 0 $^{\circ}\text{C}$ to 200 $^{\circ}\text{C}$ in a constant nitrogen flow of 50 mL min^{-1} according to the following regime. Samples were firstly cooled from room temperature to 0 $^{\circ}\text{C}$ at a rate of 10 $^{\circ}\text{C min}^{-1}$. The samples were then isothermally stabilized at 0 $^{\circ}\text{C}$ for 3 minutes, followed by heating from 0 $^{\circ}\text{C}$ to 200 $^{\circ}\text{C}$ in order to clear the thermal history of the samples. After isothermal stabilization at 200 $^{\circ}\text{C}$ for 3 minutes, the samples were cooled from 200 $^{\circ}\text{C}$ to 0 $^{\circ}\text{C}$ at a rate of 10 $^{\circ}\text{C min}^{-1}$, and the crystallization of the samples was monitored. Upon isothermal stabilization of the system at 0 $^{\circ}\text{C}$ for 3 minutes, the samples were again heated from 0 $^{\circ}\text{C}$ to 200 $^{\circ}\text{C}$ at a rate of 10 $^{\circ}\text{C min}^{-1}$, and the melting process of the crystalline phase was monitored.

Thermogravimetric analysis (TGA)

The thermal stability of the PA matrix and the PA/MWCNT and PA/MWCNT-COOH nanocomposites was determined by thermogravimetric analysis (TGA) on TA Instruments Q 500. Measurements were carried out under non-isothermal conditions by heating from room temperature to

700 °C at a rate of 10 °C min⁻¹ in a constant nitrogen flow of 60 mL min⁻¹. The change in sample mass was monitored as the temperature increased.

Thermal conductivity

Thermal conductivity of the PA matrix and the PA nanocomposites was measured by the Linseis Transient Hot Bridge (THB) device. Calibration of the device was carried out by a standard, poly (methyl-methacrylate) (PMMA). A sensor B10706 was used in the range of 0.02 – 100 W m⁻¹ K⁻¹. The standard deviation was ± 2 %. The solid sensor was placed between two samples with dimensions of 3 x 5 cm. The measurements were carried out at room temperature. The measurement time was 1 minute for each sample, whereby six values of thermal conductivity of each sample were obtained, and the arithmetic mean of the last three measurements was taken into account.

Electrochemical impedance spectroscopy (EIS)

Electrochemical impedance spectroscopy (EIS) was used in order to determine the electrical conductivity of the PA matrix and PA nanocomposites. The measurements were carried out on an apparatus consisting of a voltmeter connected to a computer, two flat electrodes in between which the samples were exchanged, and the appropriate electrode cables that linked the voltmeter and the three-electrode system located in the protective cage. The three-electrode system consisted of a working electrode, i.e., the samples of dimensions 50 x 50 x 1 mm, a reference saturated calomel electrode, and a counter-electrode. The basic principle of the measurement was based on the application of an excitation signal of a sinusoidal shape and a small amplitude of 50 mV between the reference and working electrode. The current response of the system, i.e., the current between the working and the counter-electrode was monitored. The measurements were performed in the frequency range from 100 Hz to 0.001 Hz.

Tensile test

The mechanical properties of the PA and PA nanocomposites were carried out on a universal testing machine Zwick 1445. From the samples obtained by pressing, new samples of 100 mm length and 10 mm width were made. The thickness of the samples was measured via micrometer at three different points, after which the mean thickness of the samples was calculated. The data consisting of room temperature, air humidity, sample size, and test type were entered into a computer program that manages the testing machine. The samples were placed in between the sample holding jaw at a dis-

tance of 50 mm, and subjected to uniaxial elongation at a rate of 100 mm min⁻¹ until the samples broke. Measurements were carried out at a room temperature of 25 °C. The results for each sample were presented as the average values of five measurements.

Results and discussion

Dispersion of filler in PA

In order to investigate the differences in dispersion of fillers caused by the modification of MWCNT with –COOH groups, the fracture surface of the PA composites with 5 % of both fillers, respectively, was analysed. SEM micrographs are shown in Fig. 1. On the fracture surface of nanocomposite with MWCNT filler, the areas with filler aggregates are visible, while on the micrographs of the composite with MWCNT-COOH filler, there are no visible aggregates. Modification of MWCNT with –COOH groups causes a reduction in the cohesive interactions between MWCNT, and improves adhesion interactions between the more polar MWCNT-COOH and PA matrices, and consequently allows better dispersion in the polar PA matrix.

Crystallization and melting behaviour of PA/MWCNT nanocomposites

Thermal properties of the PA matrix and PA/MWCNT nanocomposites were determined by differential scanning calorimetry (DSC) under non-isothermal conditions. Fig. 2 shows the thermograms of the cooling cycle, and the first and second heating cycles of the polyamide matrix.

In the cooling cycle, an exothermic peak was observed at a temperature around 150 °C showing the crystallization of PA. The complete crystallization of PA occurred because the rate of crystallization was higher than the cooling rate, and the material had enough time to form the crystalline structure.

In the first and second heating cycles, an endothermic melting peak was observed at 179 °C with several smaller peaks at lower temperatures. Multiple peaks were also observed in MWCNT nanocomposites with PA1010 matrix, and were explained by considering the melting-recrystallization mechanism¹⁹. As the temperature increased, the small and imperfect crystals melted and recrystallized into larger and more stable crystals. Melting of the stable recrystallized structures is visible as the main endothermic peak.

The area below the exothermic peak represents the enthalpy of crystallization, which is 69.9 J g⁻¹, while the area underneath the multiple endothermic peaks represents the melting enthalpy with the value

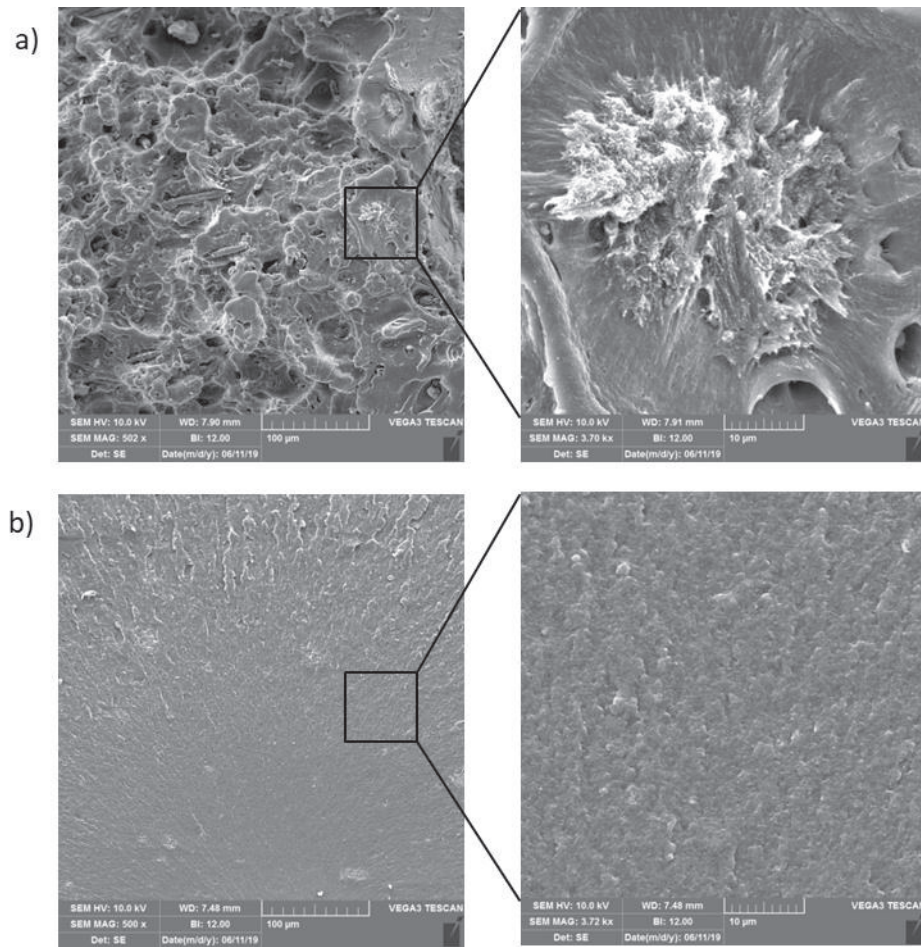


Fig. 1 – SEM micrographs of fracture surface of a) PA/MWCNT 5 % wt., and b) PA/MWCNT-COOH 5 % wt

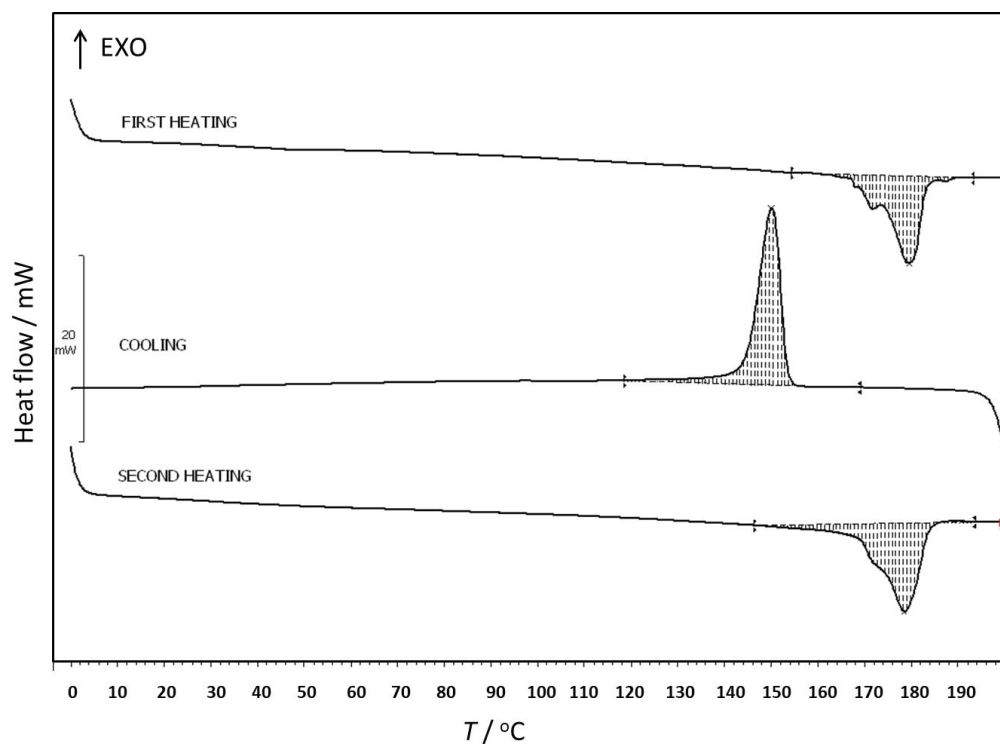


Fig. 2 – DSC thermogram of polyamide under non-isothermal conditions

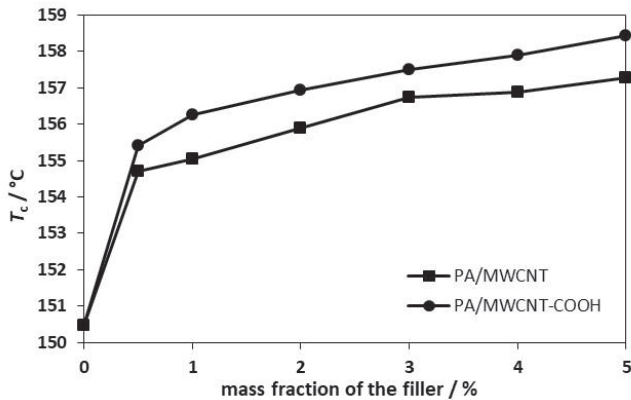


Fig. 3 – Crystallization temperature of PA/MWCNT and PA/MWCNT-COOH nanocomposites

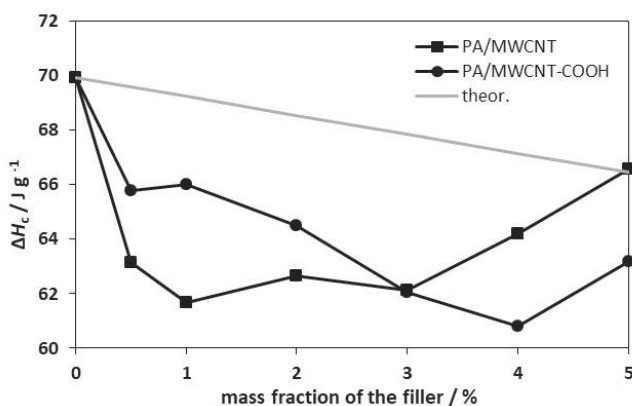


Fig. 4 – Crystallization enthalpy of PA/MWCNT and PA/MWCNT-COOH nanocomposites

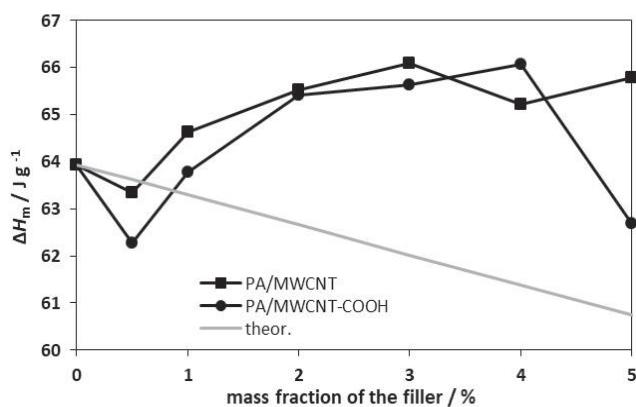


Fig. 5 – Melting enthalpy of PA/MWCNT and PA/MWCNT-COOH nanocomposites

of 63.9 J g⁻¹. It is evident that the values of enthalpy differ significantly due to the simultaneous melting and recrystallization process when increasing the temperature.

In order to analyse the influence of the MWCNT and MWCNT-COOH fillers on the crystallization of PA matrix, temperatures and enthalpies of crystallization and melting peaks of nano-

composites were analysed. The peak temperature of the crystallization determined from the DSC curve of the investigated nanocomposite systems depending on the mass fraction of the filler is shown in Fig. 3. The results showed that the addition of both fillers increased crystallization temperature to higher values in relation to PA, meaning that the fillers accelerated the crystallization of the PA matrix. The MWCNT-COOH filler accelerated the crystallization of PA more significantly compared to MWCNT fillers. Previous research also indicates an increase in the crystallization temperature by adding modified or unmodified MWCNTs into other types of PA matrices^{9–11} or polystyrene²⁰ as well as by adding nanosilica²¹ or graphene²² in PA 12.

In conclusion, carbon nanotubes act as nucleation centres and accelerate the crystallization of the PA matrix. In addition, the functionalized polar filler MWCNT-COOH creates stronger interactions with the polar PA matrix compared to the non-polar MWCNT fillers, therefore the particles are better dispersed in the matrix as the nucleation centres.

The analysis of the melting temperature showed a negligible change in the melting temperature compared to PA, since values for all nanocomposite systems were in range of 179 ± 0.4 °C (figure not shown). Consequently, MWCNT and MWCNT-COOH fillers do not affect the order or size of the PA crystallites.

The characteristic values of the crystallization enthalpy depending on the mass fraction of the fillers are shown in Fig. 4. Since the experimental values of the crystallization enthalpy for both nanocomposite systems are lower than the theoretical ones, excluding the filler fraction that does not crystallise, it can be concluded that both fillers reduce the amount of PA that can crystallise.

The possible explanation for this behaviour is that the carbon nanotubes have a nucleation effect and they accelerate crystallization of the PA 2200 matrix, however, due to their presence, the PA chains have limited motion space, therefore they interfere with the crystallization process similarly as in other types of PA matrix^{12,13}.

The values of the melting enthalpy depending on the mass fraction of the fillers are shown in Fig. 5. Almost all the values of melting enthalpy of the nanocomposites are above theoretical values, meaning that the fillers MWCNT and MWCNT-COOH enhance the crystallization of the PA matrix. Therefore, the possible explanation is that, when heated, the PA chains become mobile, which allows crystal growth. However, due to the simultaneous melting and recrystallization processes during heating, the melting enthalpy results should not be taken into consideration as an effect on the crystallization process.

Thermal stability of PA/MWCNT nanocomposites

Thermogravimetric analysis (TGA) was used in order to analyse the influence of MWCNT on the thermal stability of the PA matrix. Fig. 6 shows the TGA and DTG curves of PA. It is apparent from the shown curves, that the thermal decomposition of PA takes place in a temperature range of 300 °C to 500 °C in one step. The maximal point of the DTG curve that corresponds to the highest decomposition rate for the PA matrix is 433 °C.

In order to analyze the influence of the MWCNT and MWCNT-COOH fillers on the thermal stability of PA in the individual decomposition phases, the temperatures corresponding to 10 % (T_{90}), 50 % (T_{50}), and 90 % (T_{10}) of the mass loss were determined from the TGA curves of PA and PA nanocomposites.

The temperature corresponding to 10 % of the mass loss was defined as the start of sample decomposition (T_{90}). Fig. 7 shows an increase in temperature T_{90} by adding only 1 % of MWCNT filler, and then T_{90} decreases with a further increase in filler fraction. It is also apparent that PA/MWCNT nanocomposites have higher temperature values than PA/MWCNT-COOH. The start of thermal decomposition of the PA/MWCNT and PA/MWCNT-COOH nanocomposites varies slightly and is within the range of 406 ± 5 °C.

Temperatures corresponding to 50 % of the initial mass loss (T_{50}) are defined as indicators of the thermal stability at later stages of the decomposition. Obtained values indicate a minor change in the T_{50} of the PA nanocomposite in the range of 436 ± 5 °C (figure not shown).

Fig. 8 shows the temperature (T_{10}) at the end of the degradation process. A significant increase in temperature T_{10} is observed by adding only 1 % of both types of fillers. By further increasing the fraction of the fillers, T_{10} slightly increases. The addition of MWCNT increases T_{10} up to 12 °C, and the addition of MWCNT-COOH up to 9 °C. Therefore, it is apparent that the MWCNT filler in the final decomposition phase increases the thermal stability of the PA matrix more than the modified MWCNT-COOH filler.

In this paper, the results of the TGA analysis show that the addition of carbon nanotubes (MWCNT) increases the thermal stability of the PA matrix. Earlier investigations showed the improved thermal stability of other types of polyamide matrices by addition of MWCNT^{13–15} or graphene in PA 12 matrix²². This effect can be attributed to good thermal conductivity of MWCNT. The carbon nanotubes take on the heat that is brought during the heating, and thus slow down the degradation of the polymer matrix.

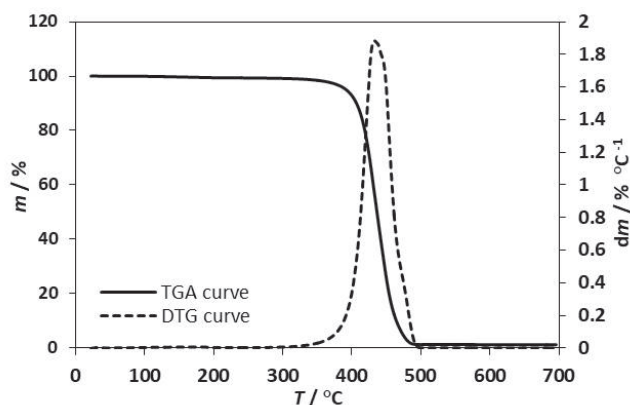


Fig. 6 – TGA and DTG curves of PA

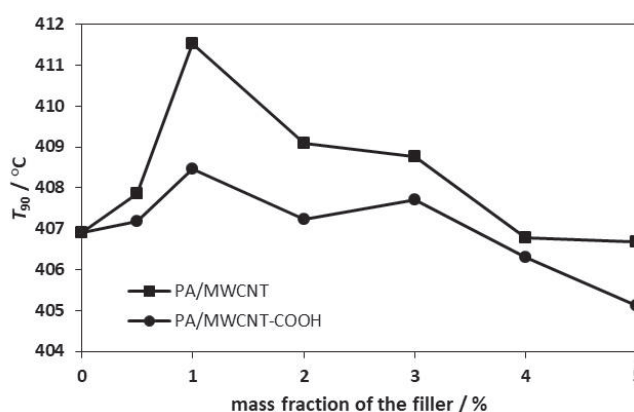


Fig. 7 – Influence of mass fraction of filler on onset temperature (10 % of mass loss) for PA/MWCNT and PA/MWCNT-COOH nanocomposites

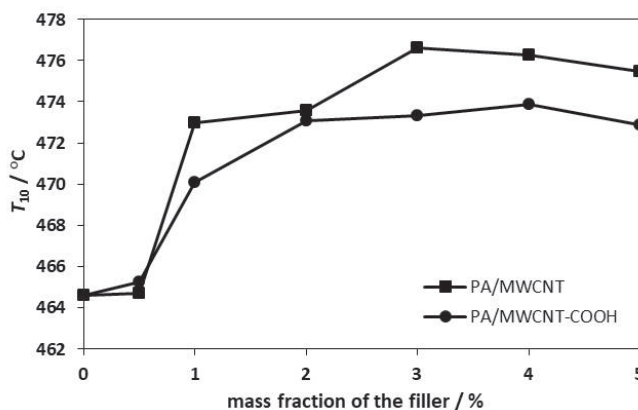


Fig. 8 – Influence of mass fraction of filler on offset temperature (90 % of mass loss) for PA/MWCNT and PA/MWCNT-COOH nanocomposites

It is apparent from previous investigations^{13–16} that the increase in thermal stability of the polymer matrix depends on the modification and the amount of MWCNT added. In this paper, by increasing the fraction of MWCNT, the thermal stability of the PA matrix had generally increased. The addition of unmodified carbon nanotubes (MWCNT) increased

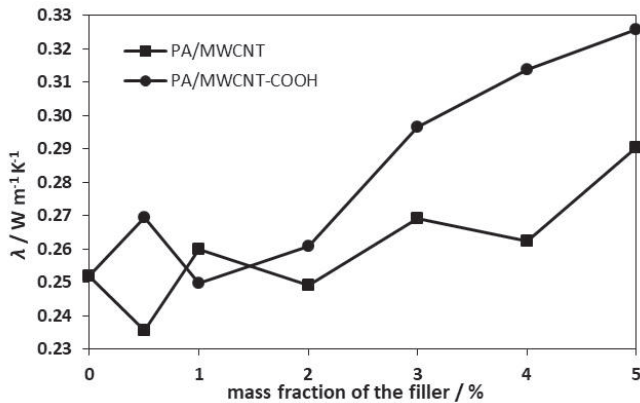


Fig. 9 – Influence of mass fraction of filler on thermal conductivity for PA/MWCNT and PA/MWCNT-COOH nanocomposites

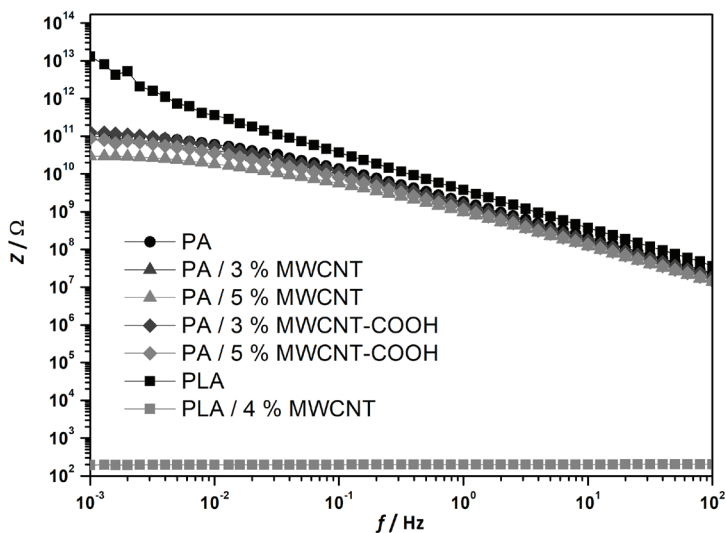


Fig. 10 – Impedance spectrum of an absolute impedance logarithm $|Z|$ of the PA and PLA matrices, and PA/MWCNT and PLA/MWCNT nanocomposites versus the logarithm of the applied frequency f

the matrix stability more than the modified ones (MWCNT-COOH). The possible explanation is that $-COOH$ groups on the carbon nanotubes adsorb water due to their polarity, and water accelerates the hydrolytic degradation of polyamide at higher temperatures¹⁴. Therefore, the thermal stability of the PA matrix, in this study, is increased more by the addition of non-polar MWCNTs rather than by the addition of polar MWCNT-COOH filler.

Thermal conductivity of PA/MWCNT nanocomposites

In order to determine the influence of multi-walled carbon nanotubes (MWCNT) on the thermal conductivity of the PA matrix, the Transient Hot Bridge (THB) method was used. Fig. 9 shows that the thermal conductivity (λ) of PA/MWCNT and PA/MWCNT-COOH nanocomposites is slightly

changed by the addition of smaller filler amounts, while at higher values of the added fillers, the thermal conductivity increases considerably.

Previous studies^{14,17} have shown that carbon nanotubes (MWCNT) increase thermal conductivity of other types of PA matrices as well, which is in line with the results obtained in this paper. Improved thermal conductivity of the polyamide matrix is attributed to good thermal conductivity of MWCNT of more than $3000 \text{ W m}^{-1} \text{ K}^{-1}$ ¹⁷. It has also been proved that the increase in thermal conductivity is dependent on the modification and the amount of MWCNT added¹⁸.

By increasing the fraction of the MWCNT added to the PA matrix, its thermal conductivity increases due to the increased number of contacts between the carbon nanotubes that create the conductive pathways. Higher conductivity is achieved by adding MWCNT-COOH filler compared to the MWCNT addition, which can be explained by stronger interactions on the filler/matrix interface and better dispersion of the filler in the matrix. Namely, MWCNT modified with the polar $-COOH$ groups enable stronger interactions with the polar PA matrix, and thus contribute to better dispersion of carbon nanotubes in the matrix¹⁸.

Electrical conductivity of PA/MWCNT nanocomposites

In order to determine the influence of MWCNT and MWCNT-COOH fillers on the electrical conductivity of the PA matrix, the electrochemical impedance spectroscopy (EIS) was used. The impedance value $|Z|$ and phase shift (θ) for each applied frequency (f) of each test sample were obtained, and some are presented in the Bode's diagram (Fig. 10). In order for a better interpretation of the impedance of the PA/MWCNT nanocomposites, measurements were also made on the polylactide matrix (PLA) and the PLA/MWCNT nanocomposite.

It is apparent from the Bode's diagram (Fig. 10) that, by decreasing the frequency, the impedance is continuously increasing in all samples, except in the PLA/MWCNT nanocomposite. The highest critical impedance, shown on the y axis at which Z has the constant value, is visible at the PLA ($\sim 1.57 \cdot 10^{13} \text{ } \Omega$) and PA ($\sim 1.07 \cdot 10^{11} \text{ } \Omega$) matrices, which is in line with expectations, since the polymers PLA and PA are non-conductive materials. However, by adding both types of the fillers, MWCNT and MWCNT-COOH, to the PA matrix, the impedance value Z changes insignificantly and remains at high value. Consequently, the reciprocal value of impedance, the admittance, which represents the conductivity of the system, also changes insignificantly, therefore no electrical conductivity

has been achieved in the PA/MWCNT system. If compared to the PLA/MWCNT nanocomposite system, it is apparent that the impedance of the PLA/MWCNT nanocomposite ($\sim 194.6 \Omega$) is reduced by almost 11 orders compared to the impedance of a non-conductive PLA matrix. Thus, by adding the MWCNT fillers to the PLA matrix, the electrical conductivity of the system is achieved.

The results obtained in this paper are inconsistent with the previous studies^{12,23,24} where significant PA conductivity was achieved by the addition of MWCNT fillers. The possible explanation for the non-conductive PA/MWCNT system is the influence of the high crystallinity of the PA matrix, which prevents close contact of the conductive MWCNTs in the polyamide that is the necessary requirement for achieving polymer conductivity.

Mechanical properties of PA/MWCNT nanocomposites

The mechanical properties of the PA matrix, PA/MWCNT and PA/MWCNT-COOH nanocomposites were tested by uniaxial elongation to determine the influence of carbon nanotubes on the nanocomposite properties. The characteristic values of the modulus of elasticity (E), yield stress (σ_y) and yield strain (ε_y) were determined from the obtained stress (σ) – strain (ε) curves.

Fig. 11 shows that, by addition of both types of MWCNT fillers, the value of the modulus of elasticity generally decreases compared to PA. It is also apparent that the nanocomposites with MWCNT fillers have higher modulus values than the nanocomposites with the MWCNT-COOH fillers.

The results of the influence of MWCNT and MWCNT-COOH fillers on yield stress (σ_y) and yield strain (ε_y) of the polyamide matrix are shown in Figs. 12 and 13. From the experimental data, it is apparent that the addition of the MWCNT filler slightly increases the stress values compared to the PA values, while the MWCNT-COOH fillers reduce the stress values. The yield strain value is increased in comparison to PA by the addition of smaller fractions of both fillers such as 0.5 %. Moreover, the strain values do not change considerably until the addition of 5 % of the fillers where the strain increases again.

In this paper, the results showed that by adding both types of MWCNT fillers in the PA 2200 matrix, the modulus of elasticity and the yield stress are reduced, but the yield strain increases, which is contrary to the results of the previous investigations^{9,13,14,25}. This behavior can be attributed to the effect of MWCNT fillers on the matrix crystallinity degree, which then affects the mechanical properties of the nanocomposites. In the section on the

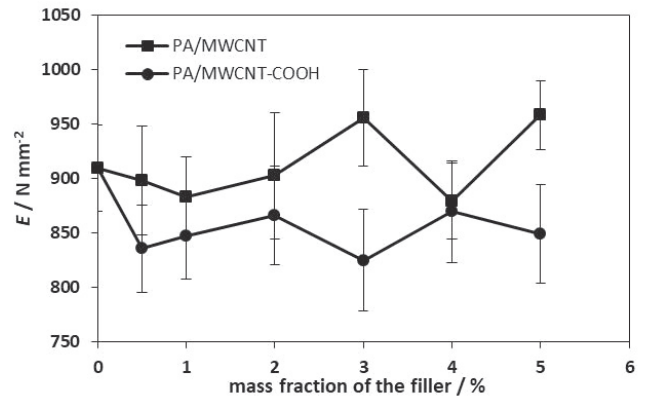


Fig. 11 – Influence of mass fraction of filler on modulus of PA/MWCNT and PA/MWCNT-COOH nanocomposites

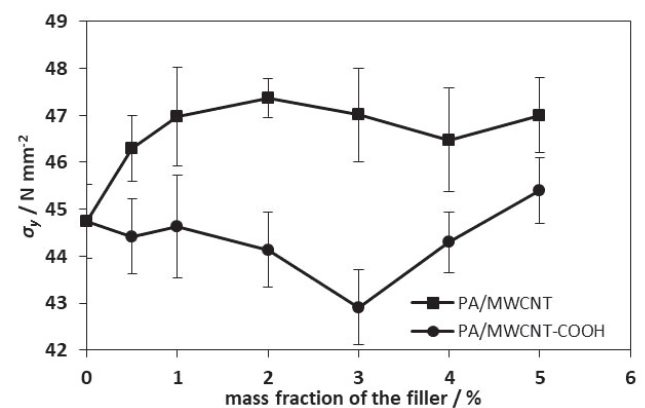


Fig. 12 – Influence of mass fraction of filler on yield stress of PA/MWCNT and PA/MWCNT-COOH nanocomposites

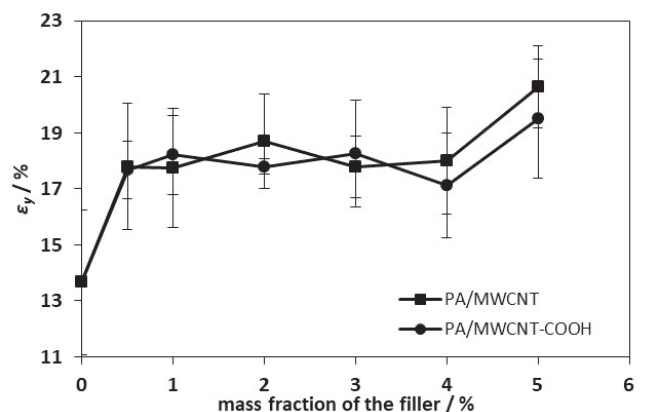


Fig. 13 – Influence of mass fraction of filler on yield strain of PA/MWCNT and PA/MWCNT-COOH nanocomposites

thermal properties of the PA/MWCNT nanocomposites, the obtained value of the crystallization enthalpy of the nanocomposite systems, which represents the crystal phase fraction, is lower than the enthalpy of the PA matrix. Thus, both types of nanofillers act by reducing the part of the matrix

that can crystallize. In conclusion, the reduced crystal fraction affects the reduction of the modulus and yield stress, and increases the deformability of nanocomposite systems, making them tougher than the PA matrix.

Conclusions

In this paper, the addition of carbon nanotubes (MWCNT) and modified carbon nanotubes (MWCNT-COOH) in the range of 0.5 wt. % to 5 wt. % in the polyamide (PA) waste powder was investigated. The results showed that carbon nanotubes (MWCNTs) acted as nucleation centres. Although the carbon nanotubes have a nucleation effect, due to their presence the PA chains have limited motion space, which interferes with the crystallization process of the matrix. The nanocomposites with MWCNT-COOH fillers more significantly accelerate the PA crystallization and exhibit higher thermal conductivity, which is due to the polar nature of the surface and the better dispersion. The thermal stability of the PA matrix increases with the addition of both MWCNT and MWCNT-COOH fillers. The higher thermal conductivity is achieved with the addition of MWCNT-COOH filler compared to the addition of MWCNT. The results imply that addition of MWCNT do not change the electrical conductivity of the nanocomposites regardless of filler modification. The results of the tensile test showed that by adding both types of MWCNT fillers in the PA matrix, the modulus of elasticity and the yield stress are reduced, but the yield strain increases. In conclusion, the addition of MWCNT fillers represents a useful approach towards the reuse of PA waste powder obtained upon SLS process.

References

1. Giannopoulos, G. I., Linking MD and FEM to predict the mechanical behaviour of fullerene reinforced nylon-12, *Composites, Part B* **161** (2019) 455. doi: <https://doi.org/10.1016/j.compositesb.2018.12.110>
2. Zhang, X., Wu, L., Wang, J., Distinct mechanical properties of polymer/polymer-grafting-graphene nanocomposites, *Macromol. Chem. Phys.* **219** (2018) 1800161. doi: <https://doi.org/10.1002/macp.201800161>
3. Zhang, L., Wang, R., Wang, J., Wu, L., Zhang, X., Mechanically robust nanocomposites from screenprintable polymer/graphene nanosheet pastes, *Nanoscale* **11** (2019) 2343. doi: <https://doi.org/10.1039/C8NR08933G>
4. Kurajica, S., Lučić Blagojević, S., Polimerni nanokompoziti in Uvod u nanotehnologiju, HDKI, Zagreb, 2017, pp 411–425.
5. Bellussi, G., Perego, C., Industrial catalytic aspects of the synthesis of monomers for nylon production, *CATTECH* **4** (2000) 4. doi: <https://doi.org/10.1023/A:1011905009608>
6. Goodridge, R. D., Tuck, C. J., Hague, R. J. M., Laser sintering of polyamides and other polymers, *Prog. Mater. Sci.* **57** (2012) 229. doi: <https://doi.org/10.1016/j.pmatsci.2011.04.001>
7. Schmid, M., Amado, A., Wegener, K., Materials perspective of polymers for additive manufacturing with selective laser sintering, *J. Mater. Res.* **29** (2014) 1824. doi: <https://doi.org/10.1557/jmr.2014.138>
8. Dotchev, K., Yusoff, W., Recycling of polyamide 12 based powders in the laser sintering process, *Rapid Prototyp. J.* **15** (2009) 192. doi: <https://doi.org/10.1108/13552540910960299>
9. Pelech, I., Kwiatkowska, M., Jędrzejewska, A., Pelech, R., Kowalczyk, I., Thermal and mechanical properties of polyamide 12/modified carbon nanotubes composites prepared via the in situ ring-opening polymerization, *Polimery* **62** (2017) 101. doi: <https://doi.org/10.14314/polimery.2017.101>
10. Phang, I. Y., Ma, J., Shen, L., Liu, T., Zhang, W. D., Crystallization and melting behaviour of multi-walled carbon nanotube-reinforced nylon-6 composites, *Polym. Int.* **55** (2006) 71. doi: <https://doi.org/10.1002/pi.1920>
11. Mahmood, N., Islam, M., Hameed, A., Saeed, S., Polyamide 6/multiwalled carbon nanotubes nanocomposites with modified morphology and thermal properties, *Polymers* **5** (2013) 1380. doi: <https://doi.org/10.3390/polym5041380>
12. Chiu, F. C., Kao, G. F., Polyamide 46/multi-walled carbon nanotube nanocomposites with enhanced thermal, electrical, and mechanical properties, *Composites, Part A* **43** (2012) 208. doi: <https://doi.org/10.1016/j.compositesa.2011.10.010>
13. Zeng, H., Gao, C., Wang, Y., Watts, P. C. P., Kong, H., Cui, X., Yan, D., In situ polymerization approach to multiwalled carbon nanotubes-reinforced nylon 1010 composites: Mechanical properties and crystallization behavior, *Polymer* **47** (2006) 113. doi: <https://doi.org/10.1016/j.polymer.2005.11.009>
14. Chen, G. X., Kim, H. S., Park, B. H., Yoon, J. S., Multi-walled carbon nanotubes reinforced nylon 6 composites, *Polymer* **47** (2006) 4760. doi: <https://doi.org/10.1016/j.polymer.2006.04.020>
15. Ribeiro, B., Nohara, L. B., Oishi, S. S., Costa, M. L., Botelho, E. C., Nonoxidative thermal degradation kinetic of polyamide 6,6 reinforced with carbon nanotubes, *J. Thermoplast. Compos. Mater.* **26** (2013) 1317. doi: <https://doi.org/10.1177/0892705712439566>
16. Li, J., Tong, L., Fang, Z., Gu, A., Xu, Z., Thermal degradation behavior of multi-walled carbon nanotubes/polyamide 6 composites, *Polym. Degrad. Stab.* **91** (2006) 2046. doi: <https://doi.org/10.1016/j.polymdegradstab.2006.02.001>
17. Yu, J., Tonpheng, B., Andersson, O., Thermal conductivity and heat capacity of a nylon-6/multi-wall carbon nanotube composite under pressure, *AIP Conf. Proc.* **1255** (2010) 145. doi: <https://doi.org/10.1063/1.3455559>
18. Han, Z., Fina, A., Thermal conductivity of carbon nanotubes and their polymer nanocomposites: A review, *Prog. Polym. Sci.* **36** (2011) 914. doi: <https://doi.org/10.1016/j.progpolymsci.2010.11.004>
19. Schick, C., Differential Scanning Calorimetry (DSC) of semicrystalline polymers, *Anal. Bioanal. Chem.* **395** (2009) 1589. doi: <https://doi.org/10.1007/s00216-009-3169-y>

20. Sun, G., Chen, G., Liu, Z., Chen, M., Preparation, crystallization, electrical conductivity and thermal stability of syndiotactic polystyrene/carbon nanotube composites, *Carbon* **48** (2010) 1434.
doi: <https://doi.org/10.1016/j.carbon.2009.12.037>
21. Chunze, Y., Yusheng, S., Jinsong, Y., Jinhui, L., A nanosilica/nylon-12 composite powder for selective laser sintering, *J. Reinf. Plast. Compos.* **28** (2009) 2889.
doi: <https://doi.org/10.1177/0731684408094062>
22. Zhu, D., Ren, Y., Liao, G., Jiang, S., Liu, F., Guo, J., Xu, G., Thermal and mechanical properties of polyamide 12/graphene nanoplatelets nanocomposites and parts fabricated by fused deposition modeling, *J. Appl. Polym. Sci.* **134** (2017) 45332.
doi: <https://doi.org/10.1002/app.45332>
23. Vankayala, R. R., Petrick, W. J. L., Cheng, K. C., Hwang, K. C., Enhanced electrical conductivity of nylon 6 composite using polyaniline-coated multi-walled carbon nanotubes as additives, *Polymer* **52** (2011) 3337.
doi: <https://doi.org/10.1016/j.polymer.2011.05.007>
24. Ferreira, T., Conceição, M. P., Pontes, A. J., Dispersion of carbon nanotubes in polyamide 6 for microinjection moulding, *J. Polym. Res.* **20** (2013) 301
doi: <https://doi.org/10.1007/s10965-013-0301-7>
25. Liu, T., Phang, I. Y., Shen, L., Chow, S. Y., Zhang, W. D., Morphology and mechanical properties of multiwalled carbon nanotubes reinforced nylon-6 composites, *Macromolecules* **37** (2004) 7214.
doi: <https://doi.org/10.1021/ma049132t>